ROBUST AEROELASTIC OPTIMISATION OF COMPOSITE PLATE WINGS SUBJECT TO PLY ORIENTATION UNCERTAINTY

Carl Scarth[1*], Pia N. Sartor[1], Jonathan E. Cooper[1], Paul M. Weaver[1], and Gustavo H.C. Siva[2]

[1]Department of Aerospace Engineering, University of Bristol
Bristol, BS81TR, UK
* Corresponding author email: cs5938@bristol.ac.uk

[2]Embraer S.A.,
São José dos Campos, São Paulo, 12227-901, Brazil

Keywords: Aeroelastic tailoring, Composite wings, Robust optimisation, Uncertainty quantification

ABSTRACT

An approach is presented for the robust stacking sequence optimisation of composite plate wings with uncertain ply orientations. An aeroelastic model is constructed using the Rayleigh-Ritz technique coupled with modified strip theory aerodynamics. Gaussian process emulators are used in conjunction with Support Vector Machine classifiers to construct a surrogate for the discontinuous and non-smooth aeroelastic instability speed, across the space of lamination parameters. The surrogate model is used to estimate the probability that instability occurs at a given design speed, which is minimised using a genetic algorithm. For each evaluation of the objective function, existing data points are reused and the surrogate is updated when required using an adaptive Design of Experiments based upon a modified Latin Hypercube. Optimised stacking sequences are compared to deterministic optima for maximum instability speed. Three layup strategies are undertaken; (i) a benchmark in which ply orientations are limited to 0°, ±45° and 90°, (ii) in which values of ±30° and ±60° are also permitted, and (iii) in which orientations are fixed to 5° increments. Improvements in reliability of at least 83% are achieved using the benchmark layup strategy, with at least 95% and 97% improvements for the second and third strategies respectively. A factor of twenty reduction in the required number of model runs is achieved by using the adaptive surrogate, though this only corresponds to a factor of four reduction in computation time due to the additional time required to fit the surrogate.

1 INTRODUCTION

Composite materials are being used to an increasing degree in aerospace structures due to a number of useful attributes including high specific strength and stiffness, and anisotropic behaviour which may be exploited to tailor properties. Aeroelasticity is concerned with the static and dynamic response of structures subject to aerodynamic loads. Aeroelastic tailoring [1-6], seeks to exploit anisotropy through selection of designs which achieve minimum-weight designs subject to aeroelastic, loads and aerodynamic design constraints. Example applications have included divergence [1] and flutter [2-4], as well as gust and manoeuvre loads [5, 6].

Computer models can represent aeroelastic behaviour to a high degree of accuracy, however, in reality all materials and processes are subject to variability. Composite materials require complex manufacturing techniques which can introduce parametric uncertainty from a number of sources including material non-homogeneity, fibre misalignment, waviness and wrinkling [7-8]. Accounting for this uncertainty by using safety margins can be overly conservative and a need for aeroelastic models which incorporate uncertainty has been identified [9]. More efficient designs can be sought through robust optimisation [10] in which the sensitivity of model outputs to uncertainty is minimised.

Numerous approaches can be taken to optimise structures under uncertainty. Reliability measures the probability of survival within the design envelope, and is often maximised or used as a constraint in a

Reliability-Based Design Optimisation (RBDO) [11]. A robust design seeks to find a compromise between minimising the variability and optimising the mean performance of the structure [10, 12]. Robust design and RBDO can be highly computationally expensive due to the number of model runs required to accurately quantify the effects of uncertainty [13]. The First Order Reliability Method (FORM) requires less computational effort due to the use of an approximate reliability index, based around a first order Taylor series expansion about the most probable parameter values [14]. Alternatively, a surrogate model [15-16] can be constructed to reduce the computational expense.

Gaussian processes can be used as surrogate models to reduce effort required for uncertainty quantification [17] and robust design [16] through interpolation of known model outputs at a small number of data points [18]. Using global Gaussian process surrogates, updated by adaptive sampling criteria [19], can further reduce the number of model runs required for optimisation [20] and reliability analysis [21]. Gaussian processes are limited to modelling smooth functions, however, they can be applied in a piecewise fashion by using classification techniques such as decision trees [22]. A thorough review of classification techniques can be found in [23].

This paper investigates the use of adaptive sampling techniques and surrogate modelling for the efficient robust optimisation of composite plate wings with uncertain ply orientations. A genetic algorithm is used to minimise the probability of aeroelastic instability at design airspeeds. A surrogate model composed of Gaussian processes combined with a Support Vector Machine classifier [23] is constructed to incorporate mode-switching behaviour between different instability mechanisms. This surrogate is updated for each evaluation of the objective function using a variant of an optimal Latin Hypercube [19]. Reliability of optimised robust and deterministic designs are compared, and efficiency of the proposed approach is compared with that of one which uses non-adaptive surrogates.

2 MODEL DEFINITION

In this paper a composite wing is idealised as a flat, rectangular, cantilever plate as shown in Figure 1. The dimensions and material properties used throughout the paper are given in Table 1. The effect of ply orientation uncertainty is included by adding an independent and identically distributed Gaussian error, with zero mean and standard deviation of five degrees, to each ply orientation.

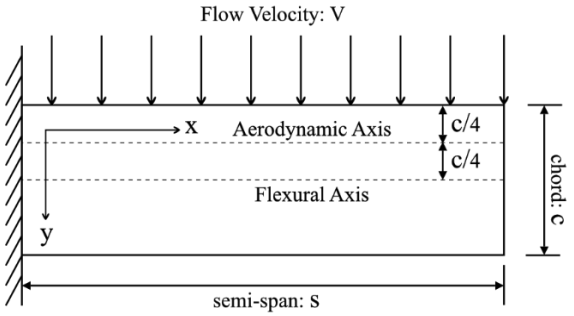

Figure 1: Composite plate geometry

Semi-span (m)	Chord (m)	E_{11} (GPa)	E_{22} (GPa)	G_{12} (GPa)	υ_{12}	ρ (kg/m^3)	Ply Thickness (mm)	Laminate Thickness (mm)
0.3048	0.0762	140	10	5	0.3	1600	0.125	2

Table 1: Dimensions and material properties used in examples

3 AEROELASTIC MODEL

The aeroelastic response of the plate is modelled using the Rayleigh Ritz method coupled with strip theory [24]. Polynomial shape functions are assumed for the out-of-plane displacement in order to approximate energy terms, which are in turn minimised. Kinetic energy of the plate is given by

$$T = -\frac{1}{2}\rho t \iint \dot{w}^2 dxdy \tag{1}$$

where ρ is the material density, t the laminate thickness, w is the out-of-plane displacement and a dotted parameter denotes a derivative with respect to time. Strain energy is given by

$$U = \frac{1}{2}\iint \boldsymbol{\kappa}^T D \boldsymbol{\kappa}\, dxdy \tag{2}$$

where $\boldsymbol{\kappa}$ is the curvature. The out-of-plane laminate stiffness D, is expressed as a linear combination of material invariants $U_{1\text{-}5}$, thickness t, and out-of-plane lamination parameters $\xi_{9\text{-}12}$ in accordance with [25]

$$\begin{Bmatrix} D_{11} \\ D_{12} \\ D_{22} \\ D_{66} \\ D_{16} \\ D_{26} \end{Bmatrix} = \frac{t^3}{12} \begin{bmatrix} 1 & \xi_9 & \xi_{10} & 0 & 0 \\ 0 & 0 & -\xi_{10} & 1 & 0 \\ 1 & -\xi_9 & \xi_{10} & 0 & 0 \\ 0 & 0 & -\xi_{10} & 0 & 1 \\ 0 & \frac{\xi_{11}}{2} & \xi_{12} & 0 & 0 \\ 0 & -\frac{\xi_{11}}{2} & \xi_{12} & 0 & 0 \end{bmatrix} \begin{Bmatrix} U_1 \\ U_2 \\ U_3 \\ U_4 \\ U_5 \end{Bmatrix} \tag{3}$$

where the lamination parameters are a function of ply orientations $\theta(u)$, defined as

$$\{\xi_9, \xi_{10}, \xi_{11}, \xi_{12}\} = \frac{3}{2}\int_{-1}^{1} \{cos2\theta(u), cos4\theta(u), sin2\theta(u), sin4\theta(u)\}u^2 du \quad \text{where } u = \frac{2z}{t} \tag{4}$$

Lift and pitching moment are applied to infinitesimal strips at the quarter chord and integrated over the span of the plate wings. The loads applied to each strip are given by

$$dL = \frac{1}{2}\rho_a V^2 c a_w \left(\theta + \frac{\dot{w}}{V}\right) dx \tag{5}$$

$$dM = \frac{1}{2}\rho_a V^2 c^2 \left(e a_w \left(\theta + \frac{\dot{w}}{V}\right) + M_{\dot{\theta}} \frac{\dot{\theta} c}{4V}\right) dx \tag{6}$$

where ρ_a and V denote the air density and velocity, c the chord length, e the eccentricity between quarter chord and flexural axis, a_w the effective lift curve slope, and θ the elastic twist. A simplified analysis is used wherein the unsteady aerodynamic derivative $M_{\dot{\theta}}$ is assumed to be constant with respect to frequency changes. Previous work has validated the use of this modified strip theory for high aspect ratio composite wings at low airspeeds through comparison with the standard Doublet Lattice approach [26]. Work done by the applied load is given by

$$\mathrm{W} = \int (-dL\delta w + dM\delta\theta)\mathrm{d}x \tag{7}$$

Application of Lagrange's equation [24] to Equations (1-2) and (7) gives the equation of motion as

$$A\ddot{\boldsymbol{q}} + \rho_a V B \dot{\boldsymbol{q}} + (\rho_a V^2 C + E)\boldsymbol{q} = \boldsymbol{0} \tag{8}$$

where A is the inertia matrix, B and C are the aerodynamic damping and stiffness matrices, E is the stiffness matrix, and $\boldsymbol{q}$ are generalised displacements. Equation (8) is solved as an eigenvalue problem to assess the stability of the wing at different air-speeds. An eigenvalue with positive real part indicates instability; this instability is flutter if the imaginary part is non-zero and divergence otherwise.

4 DETERMINISTIC AEROELASTIC BEHAVIOUR

Aeroelastic tailoring exploits changes in the characteristics of the aeroelastic stability of a structure. Different composite layups result in distinct instability mechanisms, which can be observed across the space of lamination parameters. Plots of the critical instability speed (V_{crit}) form a piecewise smooth and continuous surface, with boundaries at which the surface is either non-smooth or discontinuous. Figure 2 displays contours of instability speed with respect to different lamination parameter planes.

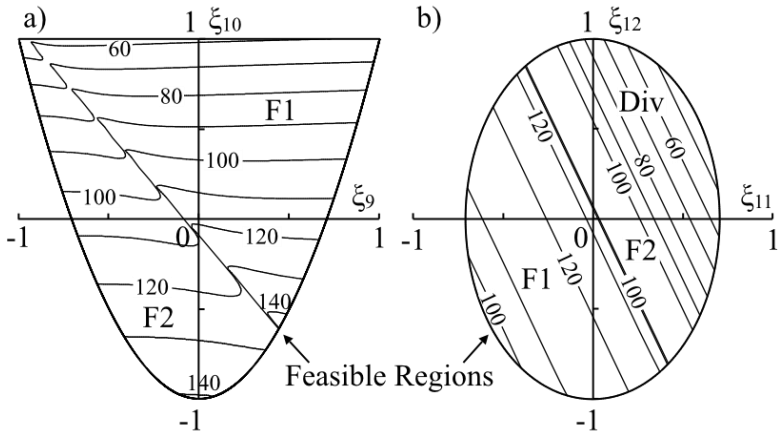

Figure 2: Contours of instability Speed (m/s) with respect to the a) uncoupled lamination parameter ($\xi_{9\text{-}10}$) plane, $\xi_{11\text{-}12} = 0$ b) bend-twist coupling lamination parameter ($\xi_{11\text{-}12}$) plane, $\xi_{9\text{-}10} = 0$

Three types of behaviour are evident in Figure 2; divergence (Div), and two flutter modes which are henceforth referred to as 'flutter 1' (F1) and 'flutter 2' (F2). Through examination of the mode-shapes, flutter 1 can be attributed to coupling of the first bending and torsion vibration modes, and flutter 2 to coupling of the second bending and first torsion modes.

4 OPTIMISATION METHOD

4.1 Benchmark Deterministic Optimisation

A benchmark deterministic design for maximum instability speed is initially obtained for comparison with the robust designs. The design space of ply orientations contains many local optima, and is often fixed to discrete values. A genetic algorithm has therefore been chosen as the most appropriate optimisation method. The MATLAB global optimisation toolbox [27] is used for this purpose.

Laminates are fixed to be symmetric with 16 plies. The ply orientations $\boldsymbol{\theta} = \{\theta_{1,\ldots,}\theta_{16}\}$, are used as design variables, which are fixed to discrete angles based upon each of following the layup strategies: (i) 0°, ±45°, and 90°, (ii) 0°, ±30°, ±45°, ±60° and 90°, and (iii) all orientations between -85° and 90° at 5° increments. Only half of the plies in each layup are parameterised as a result of the symmetry constraint, therefore the total number of design variables for all examples in this paper is eight. Ply contiguity constraints ensure no more than four plies of a given orientation are stacked together [28].

4.2 Robust Optimisation

Numerous interpretations of robust design can be found in the literature. In this paper a strategy is adopted where the probability that aeroelastic instability occurs at design air speeds is minimised [15], which is equivalent to maximising the reliability of the structure [13]. This objective can be stated as

$$\min_{\boldsymbol{\theta}} P(V_{crit}(\boldsymbol{\theta}) < V_{des}) \tag{9}$$

subject to the previously defined layup constraints. Several design instability speeds, V_{des}, are considered in order to observe the effect upon the resulting robust optima. The probability of failure is estimated using Monte Carlo Simulation as

$$\mathrm{P}(V_{crit} < V_{des}) \approx \frac{1}{n}\sum_{i=1}^{n} I(V_{crit} < V_{des}) \qquad \text{where,} \quad I(V_{crit} < V_{des}) = \begin{cases} 1, & V_{crit} < V_{des} \\ 0, & otherwise \end{cases} \tag{10}$$

This optimisation strategy is equivalent minimising the area of the instability speed Probability Density Function (PDF) which lies below the design speed.

5 SURROGATE MODEL

5.1 Surrogate Model Overview

Using Monte Carlo Simulation for reliability analysis can be computationally expensive, as this requires a large number of model runs for sufficiently accurate results. It is therefore desirable to use a surrogate model to emulate the aeroelastic instability speed at reduced computational cost. Since the surrogate is required for many evaluations of the objective function, efficiency can be improved by storing known model outputs from previous iterations. This approach is enabled through constructing the surrogate across lamination parameter space, thereby reducing the dimension and simplifying the space such that learning about the stability in one region of lamination parameters corresponds to a large number of composite layups. An overview of this adaptive surrogate is presented in Figure 3.

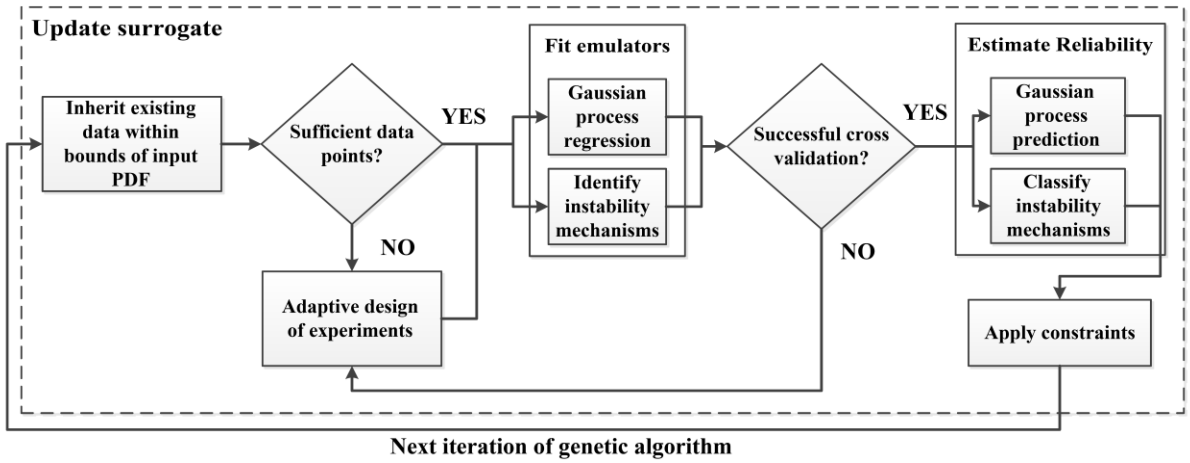

Figure 3: Surrogate model overview

Gaussian processes form the main part of the surrogate, and are described in Section 5.2. These are fitted to aeroelastic model outputs at a small number of lamination parameter training data points, and used to predict the instability speed for a Monte Carlo population of test points. A Support Vector Machine classifier is used to predict the critical instability mechanism of the test points, thereby accounting for the mode-switching behaviour. This technique is outlined in Section 5.3.

The surrogate model is updated for each evaluation of the objective function. Existing data which falls within the bounds of the current Monte Carlo population is used to form an initial set of training data points. Cross validation is used to assess whether the emulator is sufficiently accurate, and an adaptive variant of an optimised, maximin Latin Hypercube Design of Experiments is used to generate additional data points if required. This modified Latin Hypercube and its associated stopping criteria are discussed in section 5.4.

5.2 Gaussian Processes

A Gaussian process is a distribution over functions [18]. Rather than representing model outputs at each point with a deterministic value, a Gaussian process returns a Gaussian distribution. This distribution represents the uncertainty associated with the emulator fit.

The model output y, can be considered a function of input vector x, $y = f(\boldsymbol{x})$. If the value of $f(\boldsymbol{x})$ is known for a set of n training data points, $\{\boldsymbol{x}^{(1)},\ldots, \boldsymbol{x}^{(n)}\}$, uncertainty about these data points can be represented as a multivariate Gaussian distribution. The mean of this distribution can be parameterised by basis functions $\boldsymbol{h}(\boldsymbol{x})^{\mathrm{T}}$ as [17]

$$E\{f(\boldsymbol{x})|\boldsymbol{\beta}\} = \boldsymbol{h}(\boldsymbol{x})^{T}\boldsymbol{\beta} \tag{11}$$

where β is the regression weight hyperparameter, and $h(x)$ is taken as $(1, x^{\mathrm{T}})$ for linear regression.

By assuming the output is smooth, such that the value of $f(x)$ for point x gives some indication of $f(x')$ for x' close to x, the covariance function of the Gaussian process is defined as

$$cov\{f(\boldsymbol{x}), f(\boldsymbol{x}')|\sigma^2, B\} = \sigma^2 c(\boldsymbol{x}, \boldsymbol{x}')$$
$$\text{where, } c(\boldsymbol{x}, \boldsymbol{x}') = exp\{-(\boldsymbol{x} - \boldsymbol{x}')^T B(\boldsymbol{x} - \boldsymbol{x}')\} \tag{12}$$

and σ^2 is a scaling factor. The roughness matrix, B, is a diagonal matrix of length-scales which govern how much output y varies with changes to input $\boldsymbol{x}$. Maximum Likelihood Estimation gives the roughness values most likely to result in the training data.

The Gaussian process defined by Equations (11-12) is conditioned upon the output for each of the n data points. Taking prior distributions on hyper-parameters β and σ^2, a posterior distribution is obtained through Bayesian inference, and the hyper-parameters integrated out to give the student-t process [17]

$$\left[\frac{f(\boldsymbol{x}) - m^*(\boldsymbol{x})}{\hat{\sigma}\sqrt{c^*(\boldsymbol{x}, \boldsymbol{x})}}\middle| \boldsymbol{y}, B\right] \sim t_{n-q} \tag{13}$$

where $m^*(\boldsymbol{x})$, $c^*(\boldsymbol{x},\boldsymbol{x'})$ $\hat{\boldsymbol{\sigma}}$, and $\hat{\boldsymbol{\beta}}$ are defined as

$$m^*(\boldsymbol{x}) = \hat{\boldsymbol{\beta}}^T \boldsymbol{h}(\boldsymbol{x}) + \left(\boldsymbol{y} - H\hat{\boldsymbol{\beta}}\right)^T A^{-1}\boldsymbol{t}(\boldsymbol{x}) \tag{14}$$

$$c^*(\boldsymbol{x}, \boldsymbol{x}') = c(\boldsymbol{x}, \boldsymbol{x}') - \boldsymbol{t}(\boldsymbol{x})^T A^{-1}\boldsymbol{t}(\boldsymbol{x}') + [\boldsymbol{h}(\boldsymbol{x}) - H^T A^{-1}\boldsymbol{t}(\boldsymbol{x})]^T (H^T A^{-1} H)^{-1}[\boldsymbol{h}(\boldsymbol{x}') - H^T A^{-1}\boldsymbol{t}(\boldsymbol{x}')] \tag{15}$$

$$\hat{\sigma}^2 = \boldsymbol{y}^T\{A^{-1} - A^{-1}H(H^T A^{-1} H)^{-1} H^T A^{-1}\}\boldsymbol{y}. \tag{16}$$

$$\hat{\boldsymbol{\beta}} = (H^T A^{-1} H)^{-1} H^T A^{-1}\boldsymbol{y}, \tag{17}$$

noting that t is a vector of covariances such that $t_i = c(\boldsymbol{x},\boldsymbol{x}^{(i)})$, A is the training data covariance matrix such that $A_{ij} = c(\boldsymbol{x}^{(i)},\boldsymbol{x}^{(j)})$, matrix $H^T = \{\boldsymbol{h}^T(\boldsymbol{x}^{(i)}),\ldots,\boldsymbol{h}^T(\boldsymbol{x}^{(n)})\}$, $\boldsymbol{x}$ denotes a test point for which the value of $f(\boldsymbol{x})$ is to be predicted, and $\{\boldsymbol{x}^{(1)},\ldots,\boldsymbol{x}^{(n)}\}$ are the training data points for which $\{f(\boldsymbol{x}^{(1)}),\ldots,f(\boldsymbol{x}^{(n)})\}$ is known.

5.3 Classification of Instability Mechanism

A separate Gaussian process is fitted to each of the instability mechanisms identified in Figure 2 to account for the mode-switching behaviour. At the training data points the model output is known, and instability mechanisms are distinguished based upon the eigenvalue which becomes unstable.

A Support Vector Machine classifier [23, 29] is used for prediction of the instability mechanism at the test points, where the model output is unknown. A binary decision rule is used, which maps $\boldsymbol{x} \in \mathbb{R}^d$ onto $y \in \{-1,1\}$, where y = 1 corresponds to a region of the design space in which a particular instability mechanism is possible and y = -1 where it is not possible. If the data is linearly separable, a decision boundary can be defined by the hyperplane given by

$$h(\boldsymbol{x}) = \boldsymbol{w}^T\boldsymbol{x} + b \tag{18}$$

where $\boldsymbol{w}$ is a vector of weights and lies normal to the hyperplane, and b is the intercept with the origin as illustrated in Fig. 4.

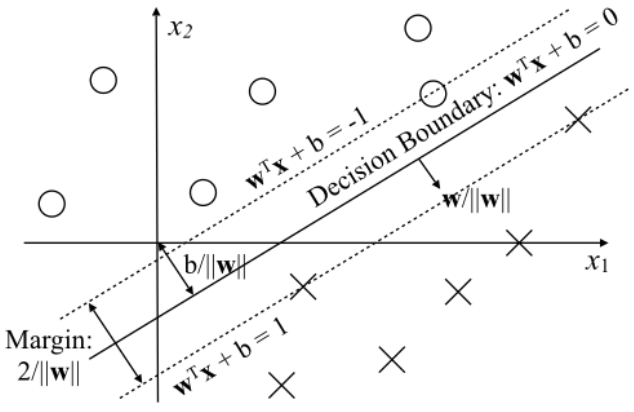

Figure 4: Linear Support Vector Machine in two dimensions

The classifier is fitted to the training data by placing the decision boundary as far as possible from each category of training data thereby maximising the margin. This approach can be shown [29] to be equivalent to the minimisation

$$min_{\boldsymbol{w},b}\ \frac{1}{2}\|\boldsymbol{w}\|^2$$
$$\text{subject to } y^{(i)}\left(\boldsymbol{w}^T\boldsymbol{x}^{(i)}+b\right)\geq 1, i=1,\ldots,n \tag{19}$$

The MATLAB function 'svmtrain' is used to fit the classifier [27]. A cubic polynomial is used to project training data onto a higher dimensional space, thereby making it easier to separate the data.

5.4 Adaptive Design of Experiments

Throughout the optimisation process, known model outputs from previous iterations are inherited for construction of the surrogate model in the current iteration. Initial training data is selected from existing samples which fall within the bounds of the current lamination parameter PDF. If no samples exist within these bounds an initial maximin Latin Hypercube is used to generate a small number of points.

Additional sample points are generated iteratively until a stopping condition is met. Since the aeroelastic model is relatively inexpensive to run, sampling criteria based upon the emulator uncertainty (e.g. [21]) are undesirable as this requires re-fitting the emulator for each new data point which is generated. A sampling technique which can generate new data points in batches is therefore preferred.

A variant of an optimised maximin Latin Hypercube [19] is adapted in order to supplement existing sample points. The process is as follows:

1) Generate a set of candidate points from a much larger Latin Hypercube than is required, combined with the existing data points.
2) For each of the *new* design points, calculate the distance to the nearest point in the candidate set.
3) Remove the point with the smallest minimum distance.
4) Repeat steps 2-3 until the desired number of points remain.

Leave-one-out cross validation is used to determine a stopping condition, such that no further data is generated once the emulator is sufficiently accurate. In this approach, one of the training data points is left out of training the Gaussian process, and the resulting emulator is used to predict the model output for this data point. This process is repeated for each of the data points and used to approximate the Root Mean Square Error (RMSE) as

$$RMSE \approx \sqrt{\frac{1}{n}\sum_{i=1}^{n}\left(y^{(i)}-m^*(\boldsymbol{x}^{(i)})\right)^2} \tag{20}$$

where m^* is the emulator mean defined in Equation (14). A RMSE of 0.25 m/s is considered sufficient accuracy, as this is of similar magnitude to the resolution of the aeroelastic model. An example plot of RMSE with emulator convergence is shown in Figure 5 for a quasi-isotropic laminate.

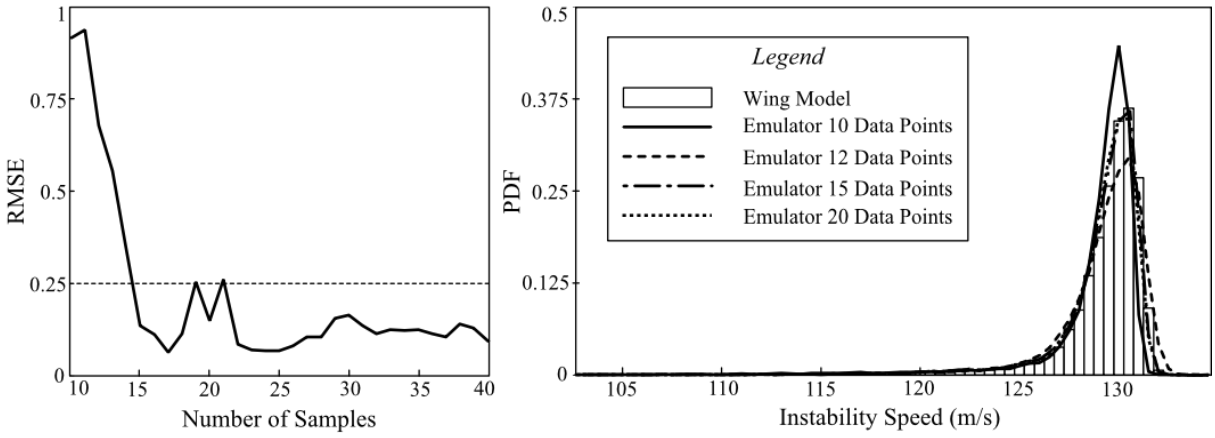

Figure 5: Convergence of an emulator with increasing number of data points, with reference to the instability speed PDF for a $[\pm 45_2, 0_2, 90_2]_S$ laminate

The long tail of the PDF in Figure 5 is a consequence of mode-switching, where the uncertainty causes a switch from divergence in the tail of the distribution to flutter which makes up the peak.

5 RESULTS

Deterministic and robust optima for the three layup strategies and design speeds of 145m/s (V_{des1}) and 150m/s (V_{des2}), are shown in Table 2 along with the number of model runs and computation time required to find the optima. Table 3 shows the nominal value, mean and standard deviation of the instability speed as well as the failure probability of each design. Figures 6-8 compare the PDFs for the critical instability speed of the optimised laminates for each of the objectives. The genetic algorithm used a population of 20 and was run for 50 generations for the first two layup strategies, and 75 generations for the third strategy due to the larger design space.

Layup Strategy	#	Objective	Layup	Model Runs	Time (s)
0°, ±45°, 90°	1	Deterministic	$[-45_2, 45_2, 0_2, \mp 45]_S$	-	-
	2	Robust, V_{des} = 145 m/s	$[-45_2, 45, -45_3, 45_2]_S$	2933	13544
	3	Robust, V_{des} = 150 m/s	$[-45_2, \pm 45, 0, 45, 0, -45]_S$	3776	18201
0°, ±30°, ±45°, ±60°, 90°	4	Deterministic	$[-45_2, 30, -45, 30_2, 45, 30]_S$	-	-
	5	Robust, V_{des} = 145 m/s	$[-45, -30, 45_2, -45, -30, -45_2]_S$	4055	17115
	6	Robust, V_{des} = 150 m/s	$[45, -30, -45_2, -30, -45, -30, 45]_S$	3583	16253
5° increments	7	Deterministic	$[-40_2, 40, 35, 40, -30, -45, 35]_S$	-	-
	8	Robust, V_{des} = 145 m/s	$[45, -40_2, -35_3, -45, -25]_S$	3808	17623
	9	Robust, V_{des} = 150 m/s	$[\mp 40, -35, -40, -45, 40, 50, -25]_S$	3670	18876

Table 2: Optimised stacking sequences for different layup strategies and objectives

#	Instability Speed (m/s)			Probability of Failure	
	Nominal	Mean	Std. Dev.	V_{des} = 145 m/s	V_{des} = 150 m/s
1	163.9	153.4	9.3	0.28	0.38
2	155.6	154.2	2.8	0.018	0.078
3	158.2	155.7	3.6	0.013	0.065
4	166.6	156.1	8.7	0.16	0.31
5	159.3	157.3	3.6	0.0007	0.027
6	160.2	158.3	3.8	0.0003	0.017
7	169.1	157.3	9.1	0.11	0.32
8	163.6	160.4	4.1	0.0001	0.015
9	162.3	159.3	3.8	0.0002	0.011

Table 3: Statistics relating to the instability speed of the optimised stacking sequences

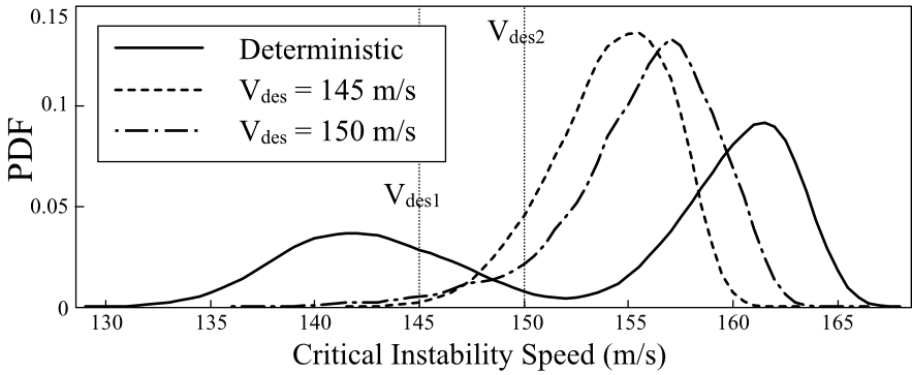

Figure 6: Comparison of instability speed PDFs for different optimised stacking sequences with 0°, ±45° and 90° plies

The required number of model runs lies between 2900 and 4100, typically taking between 13,500 and 19,000 seconds to complete the optimisation using a single core of an Intel® Core™ i7-2600s processor. Results are compared to a non-adaptive approach [30] wherein a new set of data points is generated for each evaluation of the objective function, for which a typical optimisation required 80,000 model runs taking 60,000 seconds. This constitutes a factor of 20 reduction in model runs, but only a factor of 4 reduction in overall computation time, due to the extra time required to fit the emulator in the early stages of the optimisation. It is anticipated that the reduced number of runs would be more advantageous if this approach were used with a more computationally expensive model.

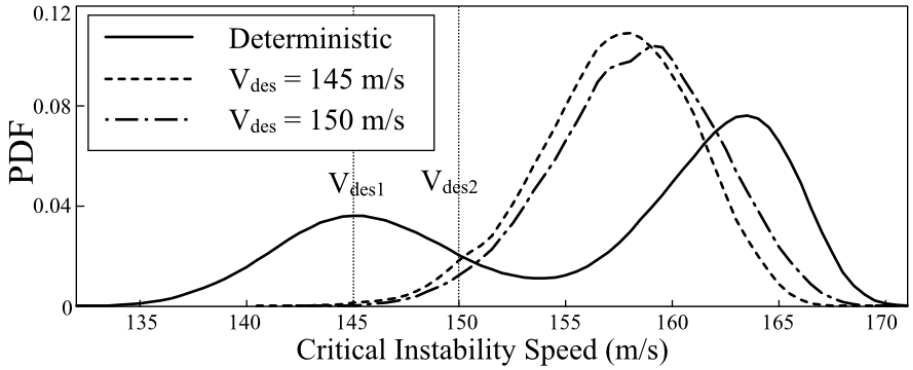

Figure 7: Comparison of instability speed PDFs for different optimised stacking sequences with 0°, ±30°, ±45°, ±60° and 90° plies

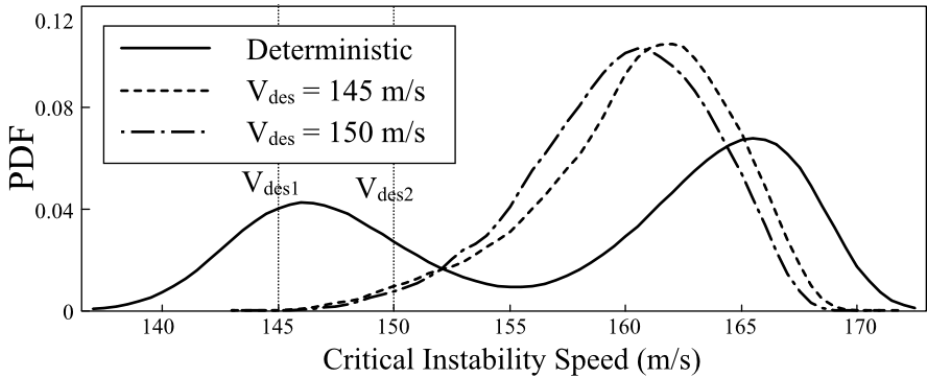

Figure 8: Comparison of instability speed PDFs for different optimised stacking sequences with potential ply orientations at 5° increments

The failure probabilities for each of the deterministic optima are notably high. It can be seen from Figure 2 that the optimal instability speed is on the boundary between two flutter modes and therefore at the edge of a discontinuity. When uncertainty is present, this results in bi-modal PDFs as shown in Figures 6-8. The high probability of switching to a flutter mode with lower instability speed, indicated by the lower peak of the PDFs, results in a high probability of failure. The robust optimisation substantially reduces the probability of failure by selecting designs further away from the discontinuity, thereby reducing the size of the lower peak of the PDF and with it the probability of a mode-switch.

The robust optimisation both reduces the standard deviation and increases the mean of the instability speed. This behaviour is atypical of robust design which is often considered to be a trade-off between mean and variance [12]. The improved average performance is due to the extent to which the mean instability speed is reduced from nominal values in the bi-modal PDFs of deterministic designs.

From Figures 6-8 it can be seen that increasing the size of the design space of ply orientations has the general trend of shifting the PDFs to higher instability speeds. This results in modest improvements to the nominal performance of deterministic designs, with much more substantial improvements to the reliability of robust designs. In comparison to the design space with only 0°, ±45°, 90° plies, the nominal instability speed of deterministic optima is increased by 1.6% through additional use of ±30° and ±60°

plies, and by 3.2% through permitting ply orientations at 5° increments. For the 145m/s robust design objective, a further reduction in the failure probability of 61% is achieved by using the second layup strategy and a reduction of 99% achieved through use of the third. For the 150m/s objective, use of strategies two and three give reductions of 74% and 83% respectively.

For the first layup strategy, different design speeds lead to significantly different robust designs due to a tradeoff between reducing the size of the lower peak of the PDF, and shifting the upper peak to higher instability speeds. No significant differences exist for the robust designs drawn from larger design spaces, as the entire PDF is shifted to higher instability speeds almost entirely eliminating instability at 145m/s. It should be noted that design number 6 performs better than number 5 for the 145m/s robust design as a result of the fact that the genetic algorithm does not guarantee finding a global optimum.

5 CONCLUSIONS

An efficient approach has been presented for the robust optimisation of composite plate wings with uncertain ply orientations. Gaussian process emulators are used in conjunction with Support Vector Machines to construct a surrogate for the discontinuous and non-smooth aeroelastic instability speed, across the space of lamination parameters. The probability of failure is estimated for different design speeds using the surrogate, and minimised using a genetic algorithm. For each iteration, previously obtained model outputs are retained by the surrogate, and additional data points are generated when required using an adaptive variant of a Latin Hypercube. Results have been determined for three different layup strategies and compared to deterministic optima to make the following observations:

- A factor of 20 reduction in the required number of model runs is achieved compared to a non-adaptive surrogate in which results are not re-used. This only corresponds to a factor of four reduction in computation time due to the increased time required to fit the emulator, however, this would be improved further if more computationally intensive aeroelastic models were considered.
- Benchmark deterministic optima have high probabilities of failure due to close proximity to a discontinuity, such that small variations in ply orientation lead to a flutter mode-switch.
- Through robust design a minimum reduction in probability of failure of 83% is achieved for laminates with 0°, ± 45° and 90° plies, of 95% when ±30° and ±60° plies are introduced, and of 97% when plies are permitted at 5° intervals. This has an added benefit of also increasing the average instability speed of the designs.
- In comparison to the first layup strategy, the second and third strategies increases nominal instability speed by 1.6% and 3.2% respectively, and improves reliability by at least 59% and 83% respectively.

ACKNOWLEDGEMENTS

The authors would like to recognise the support of the EPSRC who fund the ACCIS Centre for Doctoral Training (EP/G036772/1), Embraer S.A, and also the Royal Academy of Engineering.

REFERENCES

[1] T.A. Weisshaar, Aeroelastic tailoring of forward swept composite wings, *Journal of Aircraft*, ***18***, 1989, pp. 669-676 (doi: 10.2514/3.57542).

[2] F.E. Eastep, V.A. Tischler, V.B. Venkayya, N.S. Khot, Aeroelastic tailoring of composite structures, *Journal of Aircraft*, ***36***, 1999, pp. 1041-1047 (doi: 10.2514/2.2546).

[3] T.A. Weisshaar, R.J. Ryan, Control of aeroelastic instabilities through stiffness cross-coupling, *Journal of Aircraft*, ***23***, 1986, pp. 148-155 (doi: 10.2514/3.45282).

[4] M. Kameyama, H. Fukunaga, Optimum design of composite plate wings for aeroelastic characteristics using lamination parameters, *Computers and Structures*, ***85***, 2007, pp. 213-224 (doi: 10.1016/j.compstruc.2006.08.051).

[5] C.L. Pettit, R.V. Grandhi, Optimization of a wing structure for gust response and aileron effectiveness, *Journal of Aircraft*, ***40***, 2003, pp. 1185-1191 (doi: 10.2514/1.10821).

[6] T.U. Kim, I.H. Hwang, Optimal design of a composite wing subjected to gust loads, *Computers and Structures, **83***, 2005, pp. 1546-1554 (doi: 10.1016/j.compstruc.2005.02.002).

[7] K. Potter, B. Khan, M.R. Wisnon, T. Bell, J. Stevens, Variability, fibre waviness and misalignment in the determination of the properties of composite materials and structures, *Composites: Part A, **39***, 2008, pp. 1343-1354, (doi: 10.1016/j.compositesa.2008.04.016).

[8] S. Sriramula, M.K. Chryssanthopoulos, Quantification of uncertainty modelling in stochastic analysis of FRP composites, *Composites: Part A, **40***, 2009, pp. 1673-1684, (doi: 10.1016/j.compositesa.2009.08.020).

[9] C.L. Pettit, Uncertainty quantification in aeroelasticity: recent results and research challenges, *Journal of Aircraft, **41***, 2004, pp. 1217-1229, (doi: 10.2514/1.3961).

[10] C. Zang, M.I. Friswell, J.E. Mottershead, A review of robust optimal design and its application in dynamics, *Computers and Structures*, ***83***, 2005, pp. 315-326, (doi:10.1016/j.compstruc.2004.10.007).

[11] M. Allen, K. Maute, Reliability-based design optimization of aeroelastic structures, *Structural and Multidisciplinary Optimisation, **27***, 2004, pp. 228-242, (doi: 10.1007/s00158-004-0384-1).

[12] Z.P. Mourelatos, J. Liang, A methodology for trading-off performance and robustness under uncertainty, *Journal of Mechanical Design, **128***, 2005, pp. 856-863, (doi:10.1115/1.2202883).

[13] D.G. Liaw, H.T.Y. Yang, Reliability of uncertain laminated shells due to buckling and supersonic flutter, *AIAA Journal*, ***29***, 1993, pp. 1698-1708, (doi: 10.2514/3.10793).

[14] S.K. Choi, R.V. Grandhi, R.A. Canfield, *Reliability-based structural design*, Springer, London, 2007.

[15] A. Manan, J.E. Cooper, Design of composite wings including uncertainties: a probabilistic approach, *Journal of Aircraft, **46***, 2009, pp. 601-607, (doi: 10.2514/1.39138).

[16] R.M. Paiva, C. Crawford, A. Suleman, Robust and reliability-based design optimization framework for wing design, *AIAA Journal*, ***52***, 2014, pp. 711-724, (doi: 10.2514/1.J052161).

[17] J.E. Oakley, A. O'Hagan, Bayesian inference for the uncertainty distribution of computer model outputs, *Biometrika, **89***, 202, pp. 769-784, (doi: 10.1093/biomet/89.4.769).

[18] C.E. Rasmussen, C.K.I. Williams, *Gaussian Processes for Machine Learning*, the MIT Press, 2006, ISBN 026218253X.

[19] E. Myšáková, A. Popslíšilová, M. Lepš, Optimized design of computer experiments: a review, *Proceedings of the 12th International Conference on Computational Structures Technology (CST) (Eds. B.H.V. Topping, P. Iványi), Naples, Italy, September 2-5, 2014*, Civil-Comp Press, Stirlingshire, UK, 2014.

[20] D.R. Jones, M. Schonlau, W.J. Welch, Efficient global optimization of expensive black-box functions, *Journal of Global Optmization*, ***13***, 1998, pp. 455-492, (doi: 10.1023/A:1008306431147).

[21] B.J. Bichon, M.S. Eldred, L.P. Swiler, S. Mahadevan, J.M. McFarland, Efficient global reliability analysis for nonlinear implicit performance functions, *AIAA Journal*, ***46***, 2008, pp. 2459-2468, (doi: 10.2514/1.34321).

[22] R.B. Gramacy, H.K.H. Lee, Bayesian treed Gaussian process models with an application to computer modelling, *Journal of the American Statistical Association*, ***103***, 2008, pp. 1119-1130, (doi: 10.1198/016214508000000689).

[23] S.B. Kotsiantis, Supervised machine learning: a review of classification techniques, *Informatica, **31***, 2007, pp. 249-268.

[24] J.R. Wright, J.E. Cooper, *Introduction to Aircraft Aeroelasticity and Loads*, Wiley, New York, 2007.

[25] S. Tsai, H.T. Hahn, *Introduction to Composite Materials*, Technomic Publishing Co., Inc., Lancaster, 1980.

[26] O. Stodieck, J.E. Cooper, P.M. Weaver, P. Kealy, Improved aeroelastic tailoring using tow-steered composites, *Composite Structures*, ***106***, 2013, pp. 703-715, (doi:10.1016/j.compstruct.2013.07.023).

[27] MATLAB, Software Package, Release 2012b, The MathWorks, Inc., Natick, Massachusetts, United States.

[28] R.T. Haftka, J.L. Walsh, Stacking sequence optimisation for buckling of laminated plates by integer programming, *AIAA Journal*, ***30***, 1992, pp. 814-819, (doi: 10.2514/3.10989).

[29] N. Cristianini, J. Shawe-Taylor, *An Introduction to Support Vector Machines and other Kernel-based Learning Methods*, Cambridge University Press, Cambridge, UK, 2000.

[30] C. Scarth, P.N. Sartor, J.E. Cooper, P.M. Weaver, Robust aeroelastic design of composite plate wings, *Proceedings of the 17th AIAA Non-Deterministic Approaches Conference, AIAA SciTech, Kissimmee, Florida, USA, January 5-9, 2015*.